Solar Phys (2008) 247: 379–397
DOI 10.1007/s11207-008-9120-0

Quasi-Biennial Oscillations in the North – South Asymmetry of Solar Activity

O.G. Badalyan · V.N. Obridko · J. Sýkora

Received: 7 September 2006 / Accepted: 7 January 2008 / Published online: 27 January 2008

Abstract The north – south (N – S) asymmetry of solar activity is investigated by using the data on coronal green-line brightness and total number and total area of sunspots over the period of 1939 – 2001. Typical time variations of the N – S asymmetry are found to be consonant in these indices. Quasi-biennial oscillations (QBO) of solar activity are well recognizable in the N – S asymmetry of the examined indices. Moreover, the QBO are much better manifested in the N – S asymmetry of the individual indices than in the original (N plus S) indices. The time variations of relative QBO power are synchronous for the N – S asymmetry of various solar activity indices whereas such a synchronization is weaker for the indices themselves. It is revealed that the relative QBO power found in the N – S asymmetry of the studied indices has a negative correlation with the value of the N – S asymmetry itself. The findings indicate that the N – S asymmetry should be regarded as a fundamental phenomenon of solar activity similarly manifested in different activity indices. These findings should be taken into account when any dynamo theory of solar activity is constructed.

Keywords Coronal green line · Sunspots · North – south asymmetry · Quasi-biennial oscillations

1. Introduction

Within a classical approach to solar activity investigations it was usually assumed that all the processes on the Sun run similarly in its northern and southern hemispheres. Namely,

O.G. Badalyan (✉) · V.N. Obridko
Pushkov Institute of Terrestrial Magnetism, Ionosphere and Radio Wave Propagation,
142190 Troitsk, Russia
e-mail: badalyan@izmiran.troitsk.ru

V.N. Obridko
e-mail: solter@izmiran.troitsk.ru

J. Sýkora
Astronomical Institute of the Slovak Academy of Sciences, 05960 Tatranská Lomnica, Slovak Republic
e-mail: sykora@ta3.sk

under this assumption numerous indices of solar activity were introduced (the Wolf number, the number of polar faculae, the total radio flux, and others). Such an approach revealed the basic properties of time variations in different indices, reflecting manifestations of activity at all layers of the solar atmosphere from the photosphere to corona, in interplanetary space, and also in geomagnetic activity. Supposing identical behavior of both solar hemispheres allowed numerous theoretical concepts to be developed (*e.g.*, the Sun's differential rotation, the theory of solar dynamo, and interpretation of helioseismic measurements).

However, it gradually became clear that the northern and southern solar hemispheres operate, to a certain degree, independently. The time variations in various solar activity indices demonstrate some phase and power discordance between the two hemispheres lasting for the periods from several months to several years. Such differences between the hemispheres are commonly described as the north – south (N – S) asymmetry.

The N – S asymmetry of solar activity still belongs to the most mysterious and until now not reliably explained phenomena. Its doubtless existence disagrees to such an extent with the classical paradigm of solar activity studies that do not distinguish the Sun's two hemispheres that for a fairly long time many investigators were inclined to consider the N – S asymmetry as an artifact resulting from observational errors and statistically insignificant fluctuations of the measured quantities.

Although the N – S asymmetry has been investigated for a long time, numerous properties of this feature remain unclear, and identification of new facts reflecting different aspects of this interesting phenomenon is still in progress and valuable. The N – S asymmetry of the sunspot areas and the sunspot Wolf numbers were most widely studied. Newton and Milsom (1955) have found for the sunspot areas that the asymmetry is time variable and that these variations manifest though not quite random but still not clearly periodic character. Later, the N – S asymmetry of the sunspot indices was frequently treated by Waldmeier (1957, 1971), Roy (1977), Swinson, Koyama, and Saito (1986), Vizoso and Ballester (1990), Carbonell, Oliver, and Ballester (1993), Oliver and Ballester (1994), Nagovitsyn (1998), Li, Yun, and Gu (2001), Li *et al.* (2002), Ballester, Oliver, and Carbonell (2005), and some others.

The N – S asymmetry in the space distribution of solar flares was also studied in detail (Yadav, Badruddin, and Kumar, 1980; Knoška, 1985; Verma, Pande, and Uddin, 1987; Verma, 1987; Garcia, 1990; Bai, 1990; Ataç and Özgüç, 1996, 1998; Li, Schmieder, and Li, 1998; Li *et al.*, 2002). A number of other solar phenomena were subjected to the N – S asymmetry analysis – filaments, prominences, radio bursts, gamma rays, solar wind, coronal radiation, solar magnetic field, solar rotation, *etc.* (see, for example, Waldmeier, 1971; Howard, 1974; Hansen and Hansen, 1975; Sýkora, 1980; Rušin, 1980; Verma, 1987; Özgüç and Üçer, 1987; Tritakis, Mavromichalaki, and Petropoulos, 1988; Duchlev, 2001; Mariş, Popescu, and Mierla, 2002; Knaack, Stenflo, and Berdyugina, 2004, 2005; Gigolashvili *et al.*, 2005).

Fairly detailed reviews on N – S asymmetry studies can be found, for example, in Vizoso and Ballester (1990), Carbonell, Oliver, and Ballester (1993), Li *et al.* (2002), and Mariş, Popescu, and Mierla (2002). The extensive analysis provided many of the basic characteristics of the N – S asymmetry phenomenon. For example, quasi-periodic variations in a broad range of frequencies were revealed (see, *e.g.*, Carbonell, Oliver, and Ballester, 1993; Knaack, Stenflo, and Berdyugina, 2004, 2005; Nagovitsyn, 1998; Duchlev, 2001). The most well known of them are quasi-biennial oscillations, quasi-periodic variations with the period of 12 – 14 years, and quasi-long-period waves of 20 – 40 years. Furthermore, the presence of the N – S asymmetry leads to a discordance of active longitudes in the northern and southern hemispheres. Moreover, the active longitudes seem sometimes to be antipodal in these hemispheres (see, *e.g.*, Badalyan, Obridko, and Sýkora, 2005a, and the references to this topic in Vitinskii, Kopecký, and Kuklin, 1986).

In a number of papers the N – S asymmetries, as found in different solar activity indices, were compared (*e.g.*, Newton and Milsom, 1955; Waldmeier, 1971; Sýkora, 1980; Rušin, 1980). According to these and similar investigations an assumption can be made that the N – S asymmetry in different indices behaves similarly on different time and space scales.

In the present paper the N – S asymmetry is studied in three different solar activity indices over a relatively long period of time (1939 – 2001): the coronal green-line brightness (CGLB) I, the total sunspot area S_p, and the total number of sunspots Q. Here S_p is the real (after correcting for the projection effect) spot area in millionths of a solar hemisphere.

In our previous works (Badalyan *et al.*, 2003, 2005; Badalyan, Obridko, and Sýkora, 2005b) the following topics were treated:

(1) The space – time distributions of the N – S asymmetry derived from different solar activity indices and their mutual correlations on both short and long time scales
(2) Quasi-biennial oscillations (QBO) in the N – S asymmetry of the activity indices and their space – time distribution and comparison of the QBO in the N – S asymmetry with the QBO in the indices of activity themselves; and
(3) The relationship between the magnitude of the N – S asymmetry and the amplitude of its QBO.

The study in this paper represents some continuation and development of these topics. The results of the performed analysis indicate that the N – S asymmetry is quite important and can be an informative parameter of solar activity. It seems to represent a fundamental characteristic of solar activity, indicating a degree of accordance in processes of magnetic field generation in both solar hemispheres.

2. Observational Data

The following databases were used in our study:

(a) The coronal green-line brightness I in the line Fe XIV 530.3 nm. This is our own database. It contains observations obtained by a small world-wide network of coronal observatories and currently covers the period 1939 – 2001 (Sýkora, 1971; Storini and Sýkora, 1997; Sýkora and Rybák, 2005). Used were monthly averaged data, whose total length of sample n is equal to 756.
(b) The total area of sunspots S_p for 1939 – 2001. The monthly averaged S_p were calculated from Greenwich Observatory data available at on the Internet at http://solarscience.msfc.nasa.gov/greenwch.shtml. The Greenwich data are up to 1976, and later data are compiled by the U.S. Air Force and NOAA.
(c) The total number of sunspots Q. The monthly Q were calculated from Greenwich Observatory data accessible on the Internet, as well.

An important property common to the chosen indices is that they all describe a level of activity at specific points of the Sun's surface. Most other indices are either integrated and so related to the entire Sun (*e.g.*, the solar irradiance, the total radio flux, *etc.*) or characterize some nonstationary processes (*e.g.*, the number, intensity, and coordinates of solar flares and/or coronal mass ejections). Digitized filtergrams of the whole solar disk are not readily available and high-resolution radio maps have appeared only rather recently. All these data are beyond the scope of this paper. Another important advantage of the indices we have chosen is the length of observational data sets. The CGLB database covers, for example,

more than 5.5 activity cycles. Understandably, the data on sunspots are easily available for this period.

The CGLB represents a very appropriate index for investigation of activity and its N – S asymmetry in the solar corona. An important advantage of the I index is based on its practically simultaneous daily measurements performed during a few minutes over the whole range of solar latitudes. In fact, the measurements are performed with the step of five latitudinal degrees. Thus, our CGLB database (Sýkora and Rybák, 2005) represents a matrix of the daily I digital data recorded with steps of $\approx 13^\circ$ and 5° in solar longitude and latitude, respectively. All the data are related to a height of $60''$ above the solar limb.

The sunspots characterize activity at the level of the solar photosphere. Understandably, the sunspot indices can be used to study activity of the Sun and its N – S asymmetry in the equatorial zone only up to $\approx 30^\circ$ of latitude. In this paper we consider two sunspot indices – the total area S_p and the total number Q of sunspots. It should be emphasized that the Q quantity represents here the total number of sunspots and not the traditional Wolf number. Nonetheless, the total number of sunspots, Q, is quite an independent and intriguing index, sometimes providing better correlations with the CGLB asymmetry than, for example, the sunspot area or the Wolf number does. As follows from the studies of Kopecký and Kuklin (as quoted in Vitinskii, Kopecký, and Kuklin, 1986) the S_p and Q indices are related to the primary sunspot-formation indices in different ways.

Thus, the activity indices studied in this paper are related to different quasi-stationary manifestations of solar activity. The indices characterizing sporadic activity of the Sun are not investigated here. All the data were treated by the same technique of statistical analysis. This makes it possible to compare the results obtained for objects originating from completely different interactions of the magnetic field with the matter.

3. North – South Asymmetry in Different Solar Activity Indices

We determined the asymmetry in the standard way as $A = (N - S)/(N + S)$, where N and S are values of the corresponding activity indices for the northern and southern hemispheres, respectively. Throughout the whole analysis in this paper the monthly averaged values of all the indices were used. Commonly, the asymmetry refers to the difference between the entire northern and southern hemispheres. However, most often solar activity exhibits a clear latitude-zone structure. On that account, we found it expedient to analyze also a helio-latitudinal dependence of the asymmetry. In doing so, the N and S values are understood also as the corresponding activity indices for the latitude zones symmetrically situated with respect to the solar equator.

In Figure 1 we show variations of the N – S asymmetry on both the long (two upper panels) and short (lower panel) time scales for the three above-mentioned indices, all within the low-latitude zone $0^\circ - 30^\circ$. Curves in the upper panel are obtained by a running-averaging procedure by using the 49-month window. In this panel quasi-periodic variations of different time scales are visible. Clear similarity in the course of the N – S asymmetry is evident for all the indices in question. The paired correlation coefficients for the upper panel are rather high and are given in the second column of Table 1.

The curves in the middle and bottom panels are obtained by a certain method of spectral filtration (*i.e.*, spectral synthesis). In this method the original distribution containing n terms (where in our case $n = 756$) is subjected to a Fourier expansion consisting of $n/2$ terms. Then, an inverse summation (convolution) of a certain number of harmonics (less than $n/2$) is performed. The sum of $n/2$ harmonics describes the original sample almost exactly. Reduction of the number of harmonics, used in the inverse summation, allows us to cut the

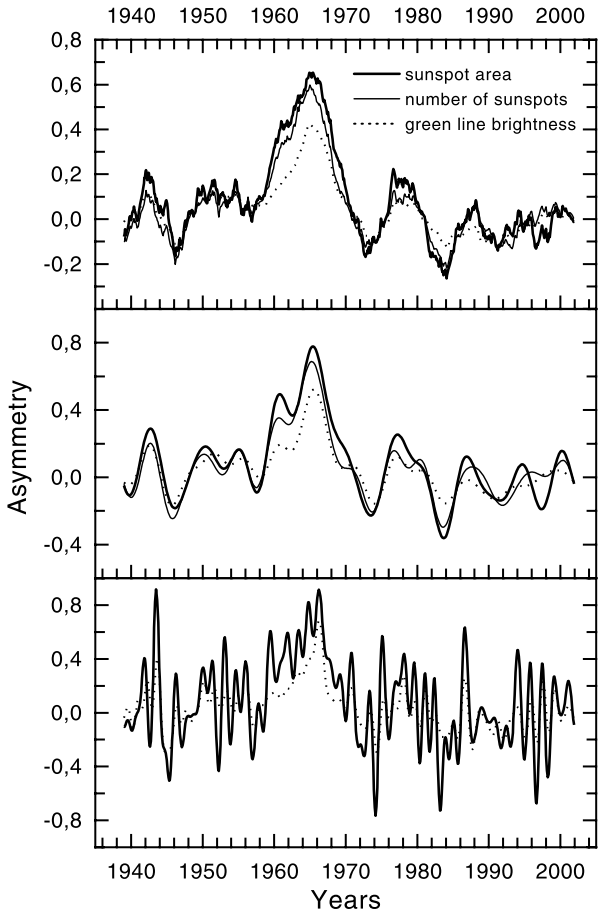

Figure 1 Time variation of the N – S asymmetry in three solar indices. Curves in the upper panel are obtained by a running-averages method by using the 49-month window. The curves in the two lower panels are obtained by a method of filtration. Only two curves are presented in the lowest panel because the sunspot number curve Q is practically identical with the S_p curve.

harmonics with periods less than the preset one. The curves in the middle panel of Figure 1 are obtained by summation of the first 15 harmonics (*i.e.*, the periods longer than 50 months are summed). The bottom panel presents the curves from summation of 50 harmonics (the periods longer than 15 months). In the bottom panel two curves are presented only – one for the sunspot area (thick line) and another one for the CGLB (dotted line). This is because the sunspot number curve Q is practically identical with the S_p curve (see also Badalyan, Obridko, and Sýkora, 2005b, where all three curves are drawn in color).

Figure 1 demonstrates very similar behavior for the N – S asymmetry on both the long and short time scales. Moreover, the method of filtration shows that a spectral distributions of the asymmetry in different indices are very similar. This follows from the fact that both the large-scale and fine-scale changes of the asymmetry are very similar for all the indices after summation of the equal number of harmonics. The paired correlation coefficients on sunspot areas versus total number of spots and sunspot areas versus green-line brightness are 0.963 and 0.928 for the middle panel and 0.930 and 0.836 for the lower panel, respectively.

In Figure 2 the N – S asymmetries of these three indices of solar activity are presented for four particular latitude zones. The curves represent the means obtained within 49-month running windows. Similarly to the lowest panel of Figure 1 here only two curves are drawn because again the Q and S_p curves practically overlap one another. One can see that the

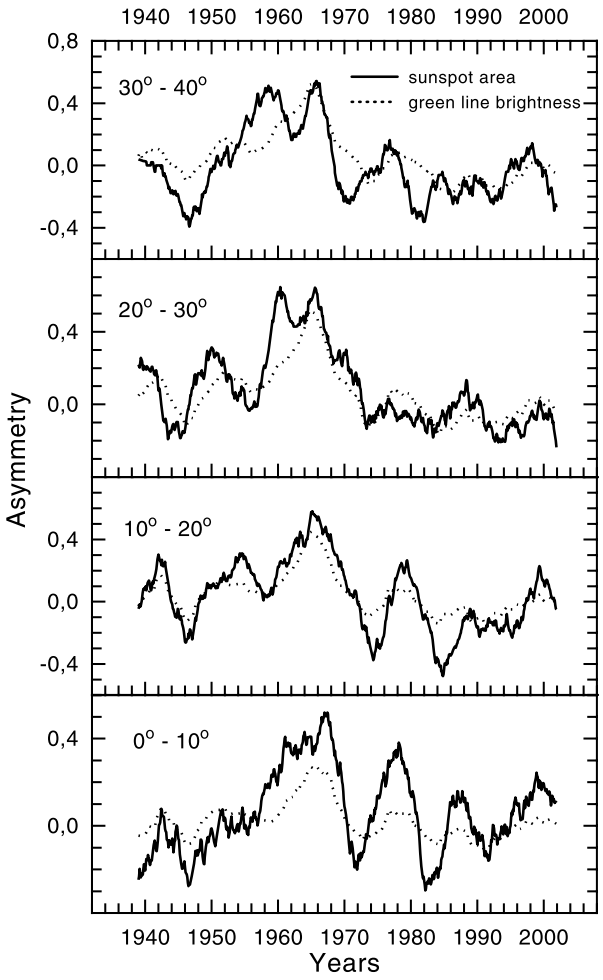

Figure 2 Long-term changes of the N – S asymmetry of two activity indices as calculated for different 10° zones. The curves are obtained by averaging within the running 49-month window.

Table 1 The paired correlation coefficients for the N – S asymmetry of three solar indices.

Paired indices	0° – 30°	0° – 10°	10° – 20°	20° – 30°	30° – 40°
$S_p - Q$	0.975	0.970	0.980	0.970	0.995
$S_p - I$	0.950	0.787	0.911	0.849	0.742
$Q - I$	0.960	0.768	0.922	0.866	0.742

general appearance of time variations in the N – S asymmetry of individual indices is mutually fairly similar whereas the differences among the latitude zones are very noticeable. The corresponding paired correlation coefficients are given in Table 1.

It is evident that the correlation of the sunspot area S_p and the sunspot number Q is, naturally, always high. The highest correlation of the asymmetry of these two indices with the asymmetry in the CGLB is observed at the latitude zones 10° – 20° and 20° – 30°. Toward equator and above 30° of latitude the correlation slightly decreases.

Figure 2 shows that the huge maximum (1958 – 1966) of the N – S asymmetry of the both sunspot indices is double-peaked at higher latitudes whereas in the CGLB asymmetry this maximum is always single-peaked. It is also noticeable from Figure 1 (upper panel) and all the panels of Figure 2 that the averaged curve of the CGLB N – S asymmetry is always considerably smooth, but the asymmetry curves obtained for the sunspot indices are still considerably indented despite the smoothing applied to the data over the 49-month window. This could be because the CGLB is more sensitive to the large-scale and more stationary processes and changes in the Sun. In contrast, sunspot activity seems to be more related to the local short-time active processes in the solar atmosphere and below.

Figures 1 and 2 demonstrate clearly that both the increases and decreases of asymmetry are essentially simultaneous in all studied indices and well correlating on both the long and short time scales. At the same time, as shown in Badalyan *et al.* (2005), and also in the present paper, the N – S asymmetry variations are almost synchronous at all solar latitudes.

4. Quasi-Biennial Oscillations in the N – S Asymmetry and in the Activity Indices

The QBO belong to the most interesting phenomena among the periodic oscillations observed in the Sun's activity. They were frequently studied (see, *e.g.*, the references in Obridko and Shelting, 2001). There are reasons to assume that the QBO are related to similar periodic processes at the base of the solar convective zone. Obridko and Gaziev (1992) showed that the QBO are distinctly visible in the N – S asymmetry of solar magnetic fields derived from Hα data. Knaack, Stenflo, and Berdyugina (2004, 2005) also revealed oscillations in this range of periods in the asymmetry of solar magnetic fields and sunspot areas. Ballester, Oliver, and Carbonell (2005) showed that a significant peak in the range of 1.44 years in the Fourier spectrum of the asymmetry (for $N - S$ value) of sunspot areas was only slightly smaller than the peaks with periods over 10 years.

Time variations shown in Figure 1 (the lowest panel) indicate that, apparently, the short-term oscillations with periods of 1.5 – 3.0 years are present in the N – S asymmetry. For a detailed analysis of the time- and latitude-dependent QBO variations a method of "spectral variation analysis" (SVAN) is used. Here, we have employed a modified SVAN, which, in contrast to that commonly used and widely described in the literature (*e.g.*, Dziewoński, Bloch, and Landisman, 1969; Thomson, 1982), includes the normalization to the standard deviation (*i.e.*, dividing by the mean-square deviation). Such normalization reduces all oscillations to a common scale and gives the sum of the squares of all amplitudes equal to 1 in each spectrum. Therefore, this enables us to compare the SVAN results of the different processes irrespectively of their units and scales.

The SVAN of any long-term set of data consists of the successive Fourier expansions realized within a running time window. This means that the Fourier expansion of the data is performed within some time window of a chosen length, then this window is shifted by some time interval and the entire procedure is repeated. The set of the resulting expansions is then used to plot a general map (the *SVAN diagram*) of the oscillation amplitudes in the time-period coordinates. In our analysis, the running window of 132 months in length was shifted successively by 12 months. The mentioned normalization to the standard deviation was done within each window. In the present paper, the amplitudes of oscillations with periods from 6 to 44 months are considered.

The SVAN-type methods have been used in various fields of science and technology for a long time. Some alternative names are often used (*e.g.*, spectral time analysis). SVAN is a natural generalization of the Fourier method. We have used this term to emphasize the

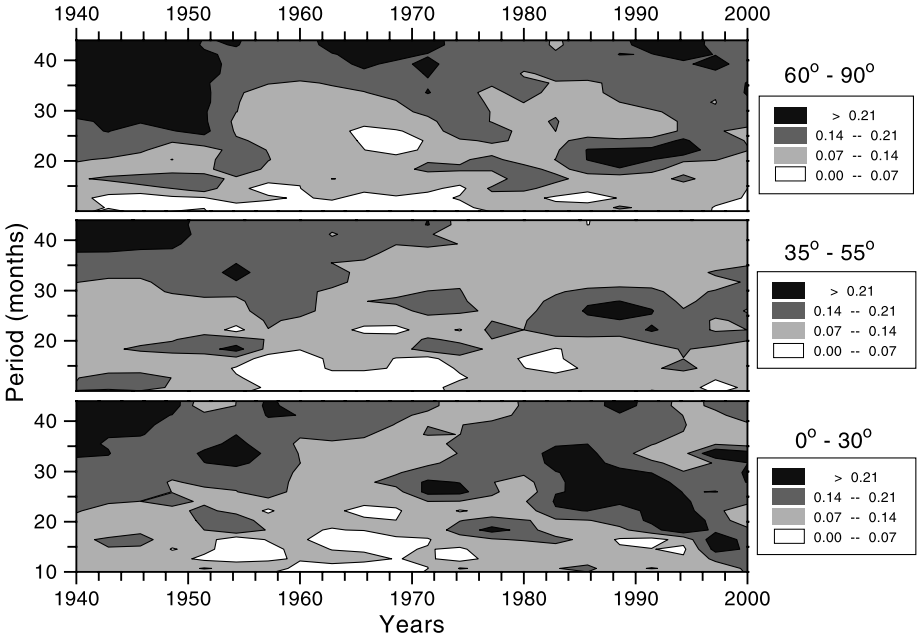

Figure 3 The SVAN diagrams for the N – S asymmetry of CGLB in three latitude zones. On this and the following SVAN diagrams, the right-hand scales show relative oscillation amplitudes.

Figure 4 The time profiles of SVAN amplitudes shown in Figure 3. The QBO amplitudes of three harmonics corresponding to the periods 18.86, 22.0, and 26.4 months were summed.

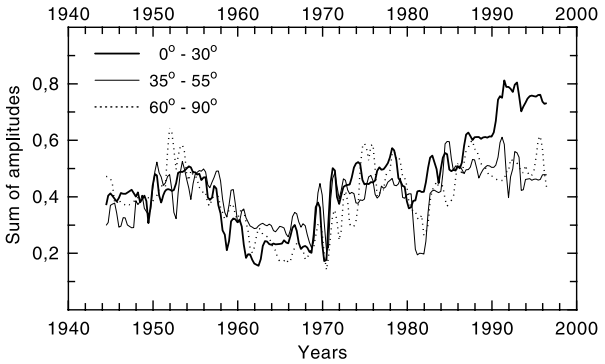

difference of the method used in our work from the traditional technique. The distinction consists in the division by the standard deviation, which allows us to compare the SVAN diagrams for considerably different indices of activity and their asymmetries. SVAN also enables a comparison of the oscillation power of various indices and their asymmetries. In addition, the normalization facilitates estimation of the reliability of the calculations (see the Appendix).

Figure 3 shows the SVAN diagrams of the CGLB asymmetry in three different latitude zones. The entire range of variations in the amplitude of oscillations is divided into four gradations, with darker shading corresponding to the high amplitudes of oscillations. These four gradations are indicated on the right-hand scale on each SVAN diagram. As follows from estimations of reliability (see the Appendix), the darkest region encircled by the contour

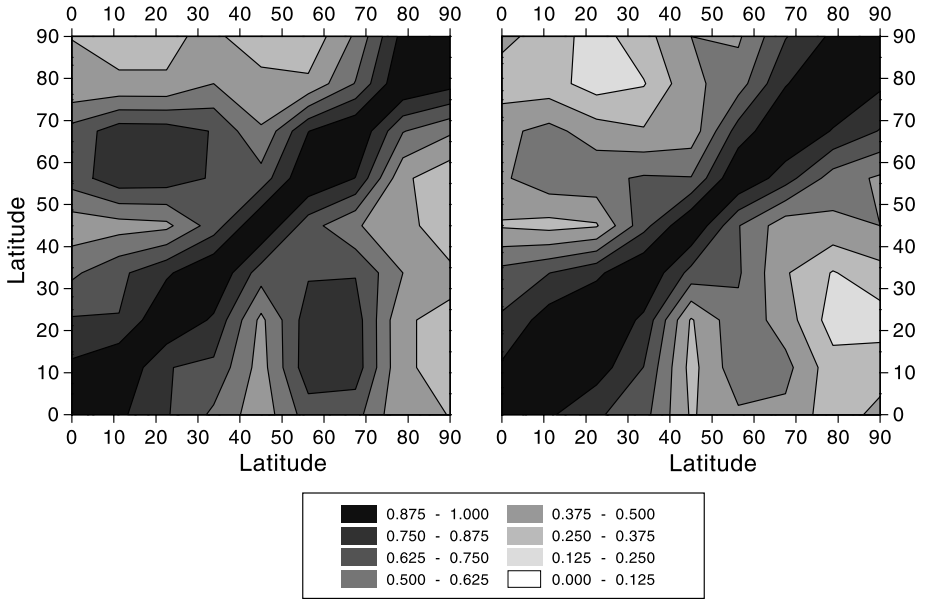

Figure 5 The paired correlation of the sums of QBO amplitudes derived from the CGLB asymmetry within 10° latitude zones. In the left map three harmonics of the QBO were summed; in the right map the sums of six harmonics (corresponding to the periods from 14.7 to 33.0 months) were used to calculate the correlation coefficients.

line of relative oscillation amplitude 0.21 corresponds to reliability $> 94.6\%$. The next contour line in this figure (0.14) corresponds to reliability 73%. Figure 3 demonstrates that the QBO (*i.e.*, the periods of 20 – 30 months) are enhanced or reduced almost simultaneously in all three latitude zones. This conclusion is also true for the much narrower 10° zones (Badalyan *et al.*, 2005). Within the equatorial zone the QBO are enhanced particularly after 1970, whereas they are most pronounced at high latitudes during the 1940s and 1950s. At the middle latitude zone the QBO are permanently less pronounced. It is worth noticing that during the 1960s, when the highest values of the N – S asymmetry were observed, the QBO were absent practically at all latitudes.

In Figure 4 we show the time profile of the sums of amplitudes of the harmonics in the QBO range for the studied latitude zones. Here, the amplitudes of three periods of oscillations, approximately corresponding to the QBO of 18.86, 22.0, and 26.4 months, are summed. Therefore, to estimate the reliability, the values on the plot must be divided by 3 and, then, compared with the data in Table 3 in the Appendix. Then, it will be readily seen that this figure confirms numerically the conclusions made on the basis of maps in Figure 3. One can see that the sums of the QBO amplitudes vary at all latitudinal zones similarly, with a correlation coefficient of ≈ 0.7. A distinctive decrease of the QBO in the middle of 1960s is visible, as well.

Figure 5 demonstrates comparison of the sums of QBO amplitudes in the CGLB asymmetry as derived within the 10° latitude zones. On these two maps the paired correlation coefficients of the QBO amplitude sums are displayed. Evidently, the diagonals between the lower left and the upper right corners represent correlation of a given zone with itself and, understandably, this is equal to 1.0. In the left map the amplitudes of those three harmonics are summed as discussed in Figure 4; the right map displays correlations of the sums of

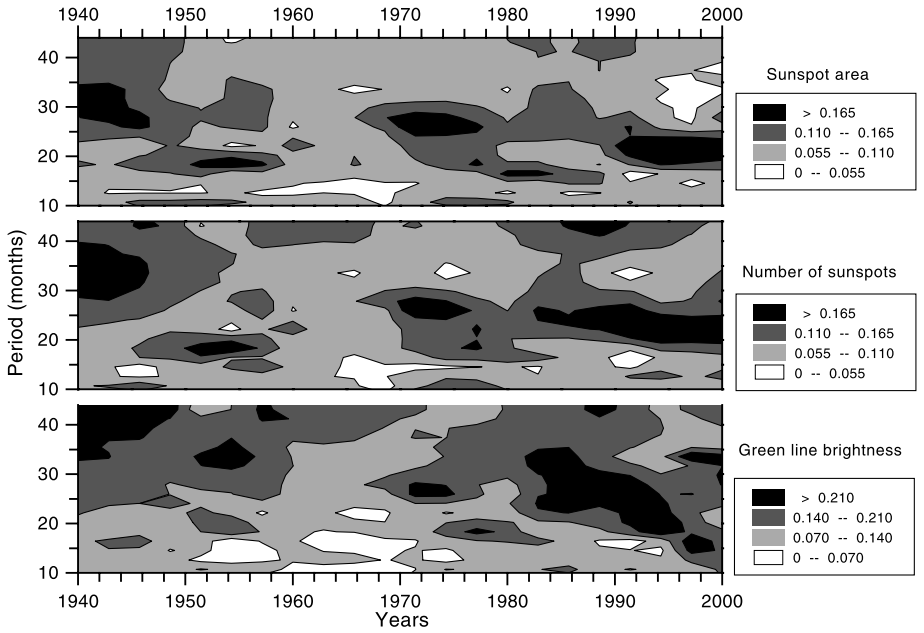

Figure 6 The SVAN diagrams for the N – S asymmetries of the sunspot areas S_p, the sunspot numbers Q, and the coronal green-line brightness I. All these are considered within the sunspot formation zone $0° - 30°$.

six harmonics within the period range 14.7 – 33.0 months. Naturally, one could expect a decrease of correlation coefficients with enlarging distance of one zone from another. However, and surprisingly, rather high correlation is observed also between relatively high latitudes of $55° - 70°$ and the low-latitude zone. When increasing the number of summed harmonics this effect becomes less pronounced but it is still recognizable. In another way, this effect can be explained also as a consequence of the substantially reduced correlation of the middle-latitude zones ($35° - 50°$) with both the lower and higher latitude zones. However, any correct interpretation of this effect remains unclear. It only can be noted that, according to helioseismic measurements, the middle latitudes are a specific region. In particular, the rotation rate in the solar convection zone at middle latitudes, unlike the other regions, does not depend on the solar radius. There are reasons to suggest that this is where the high-latitude boundary of generation of local magnetic fields is situated (Belvedere, Kuzanyan, and Sokoloff, 2000). Whether or not this phenomenon is associated with the effect revealed in our study is the subject of further investigation.

The SVAN diagrams for the N – S asymmetry of the S_p, Q, and I indices, as derived for the sunspot formation zone $0° - 30°$, are presented in Figure 6. One can see that peculiarities found for the CGLB asymmetry (Figures 3 and 4) are observed also in the asymmetry of the two other solar activity indices. Particularly, the decrease of the QBO amplitude in the 1960s and its increase during the 1970s are almost contemporary for all three indices. Understandably, the similarity of the SVAN diagrams representing the sums of QBO amplitudes for the asymmetry of S_p and Q indices seems to be quite natural, though these indices are not completely identical and relations between them are somewhat time dependent. Nevertheless, the SVAN diagrams for the QBO in the N – S asymmetry of the two sunspot indices display quite a good accordance also with the QBO in the CGLB asymmetry where a complete identity could be hardly expected.

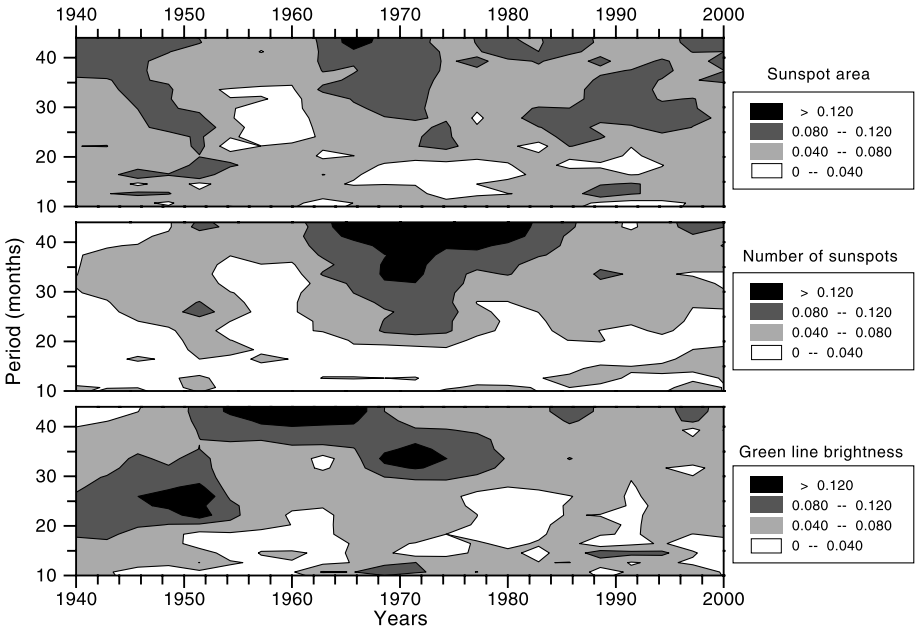

Figure 7 The same as in Figure 6, but now for the S_p, Q, and I indices themselves.

In Figure 7 we show diagrams similar to those in Figure 6 but now for the S_p, Q, and I indices themselves. It is noticeable that this figure shows much lower correspondence between the individual SVAN diagrams than is in case of the N – S asymmetry (Figure 6). However, the main point is that, being different from Figure 6, Figure 7 does not show any well-expressed QBO. Recall again that in our normalized SVAN procedure with a window of 132 months, an amplitude of 0.21 corresponds to a reliability of 94.6% and an amplitude 0.165 to a reliability of 84.4%, whereas the reliability of amplitude 0.12 does not exceed 61% (see Table 3 in the Appendix). Thus, comparison of Figures 6 and 7 allows us to state that the QBO are much better expressed in the N – S asymmetry than they are visible in the activity indices themselves. One can notice that the total range for the indices of the found amplitudes (compare the scales to the right in Figures 6 and 7) is about half that for the N – S asymmetry of indices.

The QBO amplitudes for the asymmetries of the S_p, Q, and I indices and for these indices themselves are compared in Figure 8. Here, in contrast to other figures in this paper, the sums of squared amplitudes (periods of 18.86, 22.00, and 26.40 months) are given. Recall that the sum of all the squared amplitudes is equal to unity in each spectrum. As was already pointed out, this allows us to compare a relative power of different oscillations in heterogeneous indices. The bottom panel of Figure 8 shows the sums of squared amplitudes of three QBO harmonics calculated for the total sunspot area S_p, the total sunspot number Q, and the coronal green-line brightness I. Note that the reliability of the plots in this figure is calculated in a different way, since we are dealing here with the summed squares of three amplitudes. The reliability values of this figure are given separately in Table 4 in the Appendix. Evidently, the QBO amplitudes for the indices are substantially lower in comparison with the QBO amplitudes found from their N – S asymmetries. Moreover,

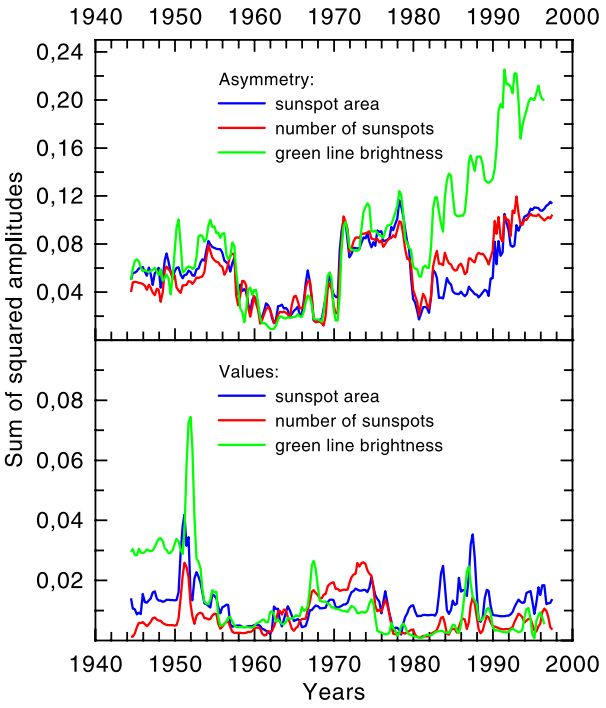

Figure 8 Time profiles of the SVAN amplitudes shown in Figures 6 and 7 showing the sums of three QBO squared amplitudes as obtained for the data within the sunspot formation zone $0° - 30°$ for the N – S asymmetry of three indices (upper panel) and for the indices alone (lower panel).

Table 2 Coefficients of the paired correlations of the sums of the squared QBO amplitudes for the N – S asymmetry and the indices themselves.

Paired indices	Asymmetry	Indices themselves
$S_p - Q$	0.88 ± 0.02	0.56 ± 0.05
$S_p - I$	0.67 ± 0.04	0.47 ± 0.05
$Q - I$	0.85 ± 0.02	0.26 ± 0.06

coefficients of the paired correlations between the sums of squared QBO amplitudes in the indices alone are also considerably less (see the last column in Table 2).

Table 2 gives the coefficients of the paired correlations between the sums of the squared QBO amplitudes for the N – S asymmetry and the indices themselves, as derived for the sunspot formation zone $0° - 30°$.

Table 2 convincingly demonstrates that the coefficients of the paired correlation are statistically significant for the N – S asymmetry comparisons only. For the indices themselves the correlation coefficient is significant in the first line only, that is, in the case of physically very related indices S_p and Q. At the same time, the sums of the squared QBO amplitudes in the N – S asymmetry for the seemingly unrelated (in the physical sense) indices I and Q show a correlation of 0.85.

In summary, our study in this section shows that the long-term increases and decreases of the QBO take place more or less synchronously in the N – S asymmetry of the three investigated indices and that the QBO are much better expressed in the N – S asymmetry of the indices than in the indices themselves.

Note that the existence of QBO in the asymmetry can be inferred, for example, from the autocorrelation analysis carried out by Rybák and Sýkora (2006). The autocorrelation

curves display secondary maxima in the time intervals when QBO are enhanced. These maxima correspond to a lag equal to the mean oscillation period of QBO. The work of these authors indirectly confirms the reliability of our results.

5. Relation between Magnitude of the N – S Asymmetry and Amplitude of Its QBO

In Figure 9 the latitude – time distributions of the CGLB asymmetry (upper panel) and the sum of the QBO amplitudes (lower panel) are presented. The amplitudes of three periods of oscillations, approximately corresponding to QBO periods of 18.86, 22.00, and 26.40 months, were summed. This figure demonstrates the long-term and large-scale variations of the asymmetry and of the sum of amplitudes. To construct the upper panel half-yearly-averaged values of the N – S asymmetry in 10° latitude zones were used. For the same zones also the sums of amplitudes were calculated to construct the lower panel. The upper panel of Figure 9 shows that the large-scale variations of the asymmetry occur almost simultaneously at all latitudes, creating rather broad vertical bands in the map. One can notice that until approximately 1970 the solar corona in the northern hemisphere was brighter than in the southern one. After 1970 the southern hemisphere began to dominate though the asymmetry is less pronounced there. In the lower panel a number of wide vertical bands are seen as well, indicating that during particular time intervals the QBO in the CGLB asymmetry are strengthened or reduced simultaneously at a wide range of solar latitudes. A remarkable strengthening of the QBO after 1970 is also very visible. Consequently, comparison of the two panels in Figure 9 allows us to point out a general large-scale anticorrelation between the CGLB asymmetry and the power of its QBO: Apparently, these two panels seem to exhibit pretty well the "positive/negative" appearance of a photographic image.

In Figure 10 this conclusion is demonstrated more directly. The time profile of the asymmetry values and the sums of QBO amplitudes, both averaged over all latitudes of Figure 9, are presented. The points of the lower curve denote the yearly averaged values of the N – S asymmetry, whereas the points of the upper curve represent the sum of QBO amplitudes obtained by the SVAN (where a 132-month window and a 12-month successive shifting of it were used). The thick lines were obtained by the method of filtration (see description earlier) and harmonics with only periods more than 6.6 years were summed. Figure 10 clearly shows that almost any large-scale long-term increase in the asymmetry corresponds to the decrease of its QBO power and, conversely, almost any decrease in the N – S asymmetry is accompanied by an increase of its QBO power.

In Figure 11 the relation between the sum of QBO amplitudes in the asymmetry and the magnitude of the asymmetry itself is plotted for the three studied indices over the latitude zone 0° – 30°. Here, each point on the graph denotes the N – S asymmetry averaged within each successively shifted SVAN window. This figure shows that for each index a negative correlation between the relative sum of the QBO amplitudes and the N – S asymmetry magnitude is observed.

In CGLB the effect of the negative correlation exists at all latitude zones. A detailed latitude dependence of this anticorrelation is shown in Figure 12. The highest correlation coefficients occur in the 10° – 20° and 60° – 70° zones. These two latitude bands are separated by a narrow 40° – 50° zone, where the correlation coefficient is distinctly lower. Namely, close to this zone the highest values of the CGLB asymmetry are found in the period 1965 – 1968 (see, *e.g.*, the upper panel of Figure 9). Note also that the 40° – 50° zone represents a boundary separating the regions of the low-latitude local magnetic fields from the large-scale polar fields.

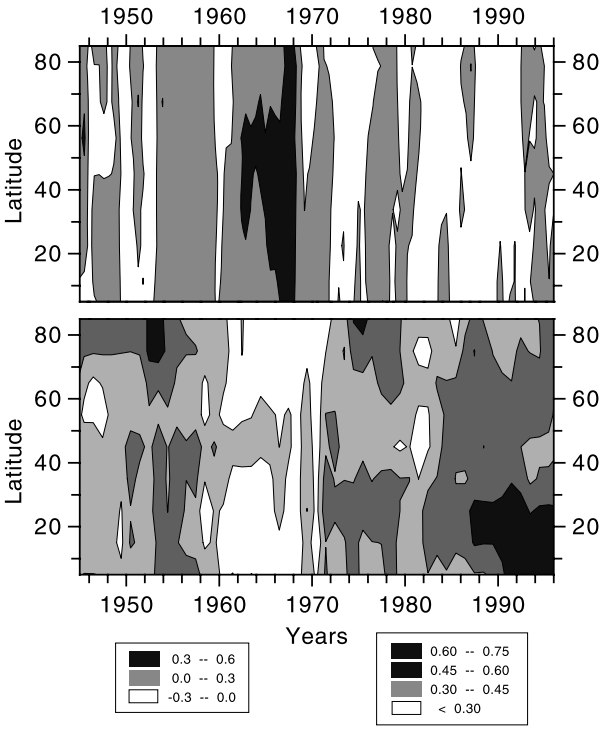

Figure 9 Time – latitude distributions of the CGLB asymmetry (upper panel) and that of the sums of its three QBO amplitudes (lower panel).

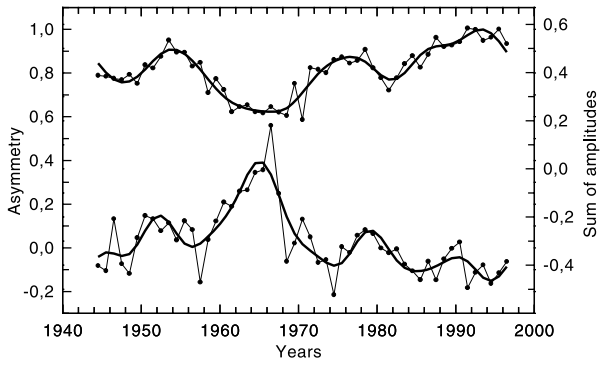

Figure 10 Time profiles of the N – S asymmetry in CGLB (upper curve) and of the sums of its QBO amplitudes (lower curve). Both thick curves were obtained by a method of filtration from the averaged data over the entire range of solar latitudes (thin broken lines).

The fact that the relationships shown in Figure 11 hold even in the time intervals where the southern hemisphere dominates (*i.e.*, the N – S asymmetry is negative) appears somewhat strange. It would be more natural to observe such a relationship between the absolute values of the asymmetry and the QBO power. Since during 1939 – 2001 there were practically no periods with the remarkably distinctive negative N – S asymmetry, an investigation of this problem was treated by using a long series data on the areas and total numbers of sunspots covering 1874 – 2002 (Badalyan and Obridko, 2003). It was found that, indeed, the absolute value of the N – S asymmetry is the determinative parameter and, consequently, that the QBO power decreases in the regions of both the negative and positive asymmetries (see Figure 4 in Badalyan and Obridko, 2003).

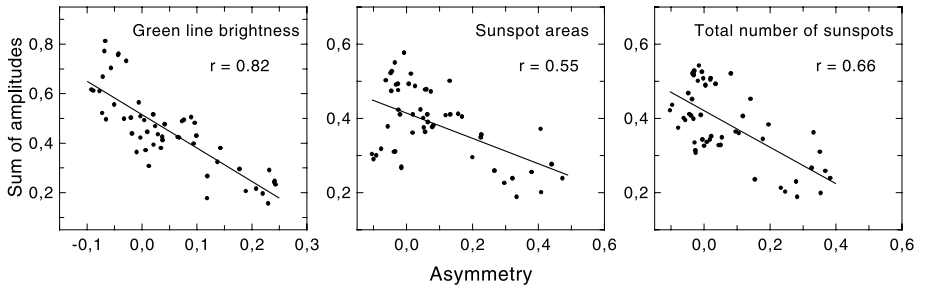

Figure 11 Anticorrelation between the sums of three QBO amplitudes in the N – S asymmetry of the three studied indices and their averaged asymmetry in each running SVAN window.

Figure 12 The latitude dependence of the negative correlation coefficient between the CGLB asymmetry and the sum of three QBO amplitudes.

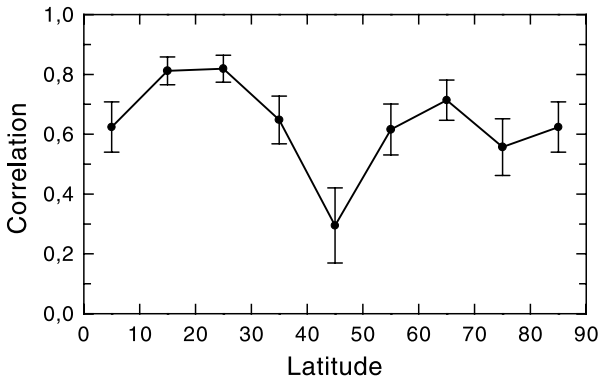

6. Conclusions

We have analyzed the N – S asymmetry A using three different indices characterizing solar activity at different levels of the solar atmosphere (the coronal green-line brightness I, the total sunspot area S_p, and the total sunspot number Q). The following main results were obtained:

1. Similar time variations on both the short (1.5 – 3.0 years) and long (≈12 years) time scales are identified in the N – S asymmetry of all studied indices within the sunspot formation zone 0° – 30°. Activity in the northern hemisphere dominated during the first half of the studied period (with a well-pronounced maximum in 1964 – 1966) but later the southern hemisphere was somewhat more active. It is shown that the spectral distributions of the N – S asymmetry of different indices are very similar.
2. Quasi-biennial oscillations in the N – S asymmetry of all indices were detected and analyzed. The spectral variation analysis method was applied in that procedure. Existence of long time intervals of the steady enhancements or weakening of the QBO power, almost simultaneous over a broad range of solar latitudes, is demonstrated.
3. Within the sunspot formation zone 0° – 30° specific features of the QBO variations in the N – S asymmetry of all indices are very similar. It is revealed that the QBO are much better expressed in the asymmetry of the indices than in the indices themselves. Also the QBO amplitudes found in the N – S asymmetry of indices correlate mutually much better than the QBO amplitudes in the indices alone do.

4. Manifestations of the QBO in the N – S asymmetry of three studied indices, particularly those in the coronal green-line brightness, appear to be in antiphase with the magnitude of the N – S asymmetry itself. This effect is, in fact, evident for all the three studied indices over the whole range of solar latitudes, reduced distinctly only at the range of 40° – 50°.

Generally speaking, the nature of the N – S asymmetry of different solar activity indices remains unexplained. As a rule, the most widespread dynamo theories do not consider the N – S asymmetry, assuming completely identical behavior of activity in both solar hemispheres. Nevertheless, investigation performed in our present paper strengthens an idea that generation and manifestations of solar activity proceed, to a large extent, independently of the Sun's two hemispheres and are governed by laws of differential rotation and meridional circulation specific for a given moment in each of the hemispheres. Because, however, activity in the solar hemispheres exhibits general temporal and energetic coincidence of the cyclic variations, one can assume that some currently unknown mechanism can exist that determines the actual degree of similarity in the evolution of active processes in the two hemispheres. This mechanism seems to exist, apparently, outside of the activity generation and is independent of it. Probably, the N – S asymmetry may represent a quantitative measure reflecting the properties of such a mechanism.

Appendix: Reliability of SVAN Diagrams

Evaluation of reliability of the Fourier spectrum is no easy task. In fact, we must determine whether one or another maximum on the SVAN diagram is true or reflects random fluctuations in the white-noise spectrum associated with the finiteness of the realization.

Actually, the SVAN diagrams of the white noise also have maxima, which can be comparable in magnitude with those observed on our experimental SVAN diagrams. We have analyzed 20 realizations of the white noise, each containing 756 numbers, which corresponds to the length of our monthly data series. For each realization, we have calculated a SVAN diagram using the same program and parameters as we did when analyzing the observational data (see Section 4). An example is shown in Figure 13.

One can see that the amplitudes are not large; however, they are comparable with the values on the SVAN diagrams for the activity indices (see Figure 7). Naturally, the appearance of larger amplitudes cannot be ruled out, but the chance of it is quite low.

In Figure 8, we have shown also the time variation of the sum of squared amplitudes of three harmonics in the QBO range. A similar plot for three random white-noise realizations is represented in Figure 14. Sometimes, one can observe relatively large sums of squared amplitudes but, as seen in the following, their probability is not high.

To evaluate reliability of the SVAN diagrams, we have considered the power spectrum (*i.e.*, the spectrum of sums of squared amplitudes) of the white-noise harmonics. It turned out that the problem could be simplified significantly by normalizing to the standard deviation. It is well known that the power spectrum of the white noise is constant (*i.e.*, $p_k = p_0$). In a general case, the value of p_0 depends on a particular character of the spectrum and scale of the signal. However, with the normalization proposed here, $\sum p_k = Np_0 = 1$. Thus, the mean value of the Fourier power spectrum of random numbers is zero (or undefined), and for a realization of finite length N, $p_0 = 1/N$.

If the Fourier coefficients are normally distributed random quantities, the distribution of squares of these coefficients is determined as χ^2 with two degrees of freedom (Jenkins and Watts, 1968), that is, χ^2_2. To determine the 95% confidence level, we can simply multiply

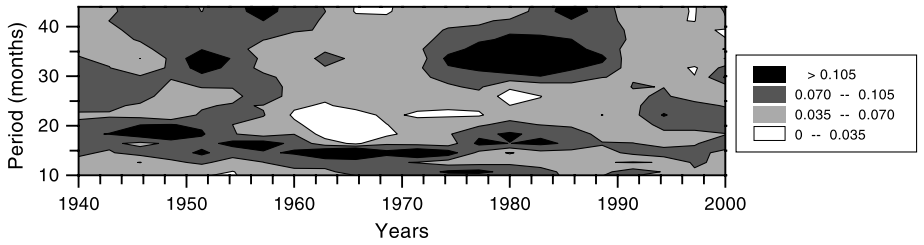

Figure 13 SVAN diagram for the white noise.

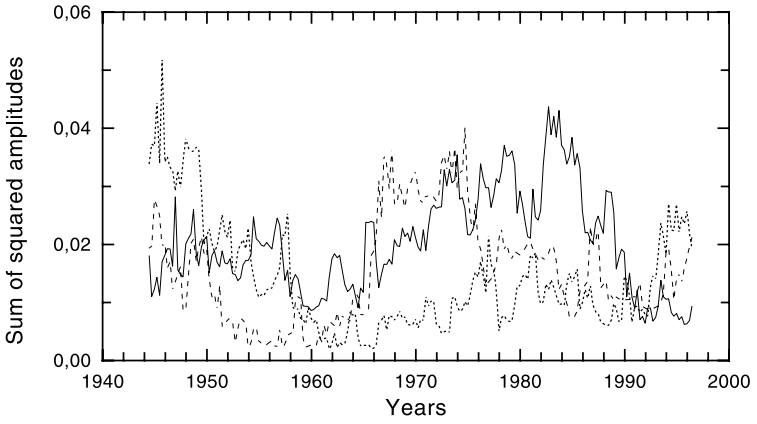

Figure 14 Time variation of the sum of squared amplitudes of three harmonics in QBO range for three random white-noise realizations.

the original white-noise spectrum by the corresponding χ_2^2 (Gilman, Fuglister, and Mitchell, 1963; Jenkins and Watts, 1968; Chatfield, 1989).

Let the probability of coincidence of this value in the power spectrum under examination with the white-noise spectrum be denoted as $\alpha[\%]$. Then,

$$\alpha[\%] = 100 \exp\left(\chi_2^2/2\right) = 100 \exp\left[-\left(x_k^2\right)N/2\right], \tag{1}$$

and the confidence (*i.e.*, probability of rejection of the hypothesis of "noise" origin of the given harmonic) is $(100 - \alpha[\%])$. Note that this expression comprises the squared amplitude of the corresponding harmonic. This should be taken into account when examining Figures 3, 6, 7, and 13, which represent the amplitudes of the harmonics rather than their squared values. Note also that Figure 4 shows the sums of three amplitudes. To analyze the confidence, the values on the plot must be divided by 3 and, then, compared with the tabulated data (Table 3).

Sometimes, we analyze squared amplitudes (*e.g.*, Figures 8 and 14 represent the sums of squared amplitudes of three harmonics), and this is taken into account in our reliability estimates (Table 4).

Heretofore, we have discussed the reliability of each particular point on the SVAN diagrams and plots. Estimating the reliability of the spectrum as a whole is a much more intricate problem, which can be defined as follows: What is the probability that two similar

Table 3 Reliability of contour lines on the SVAN diagrams with $N = 132$ points in the window.

Amplitude	Reliability (%)
0.21	94.6
0.165	84.4
0.140	73
0.120	61

Table 4 Reliability of the magnitudes in Figures 8 and 14.

Amplitude	Reliability (%)
0.20	98.6
0.14	95.6
0.12	92.9
0.08	82.8
0.02	33.4

spectra of the white-noise realization may appear? Obviously, the theoretical correlation coefficient for the spectra of two infinite white-noise realizations is zero. In the case of using, as we do, a finite realization and a moving window of finite length, the correlation coefficient differs from zero but is very small: The mutual correlation coefficients for the relations illustrated in Figure 14 are -0.17, -0.04, and 3.2. We have calculated 190 versions of pair combinations of the white noise and obtained the correlation coefficients as high as shown on the top panel of Figure 8 (Table 2) in less than 3% of the cases. Therefore, the alternative hypothesis that the original realizations of the observed asymmetry values may be random fails with 97% probability because of the high correlation of the spectra on the SVAN diagram (Figure 6) and the top panel of Figure 8.

Thus, the reliability of our results is ensured by normalization to the standard deviation of all data used for our calculations. This means that the obtained Fourier coefficients show directly what fraction of the integral dispersion (*i.e.*, of the power integrated over all frequencies) in each window is accounted for by a given harmonic. It is to be noted that the standard Fourier methods do not involve division by standard deviation, in which case the reliability of the Fourier spectra and SVAN diagrams is difficult or impossible to estimate.

Nowadays, the SVAN-type methods are treated with a certain skepticism. They have not been frequently used in the past 20 years, with preference being given to wavelets. However, it was shown long ago that the coefficients do not virtually depend on the length of the window if the Fourier method is used correctly. This means that the window should be much larger than the sought periods and that frequencies below the Nyquist frequency and that are too close should be excluded from consideration. These conditions are fulfilled in our work.

Acknowledgements This research was supported by the Russian Foundation for Basic Research (Project No. 05-02-16090) and by the Slovak VEGA Grant No. 2/7012/27.

References

Ataç, T., Özgüç, A.: 1996, *Solar Phys.* **166**, 201.
Ataç, T., Özgüç, A.: 1998, *Solar Phys.* **180**, 397.

Badalyan, O.G., Obridko, V.N.: 2003, In: Makarov, V.I., Obridko, V.N. (eds.) *Climatic and Ecological Aspects of Solar Activity*, Glav. Astron. Obs. Ross. Akad. Nauk, St. Peterburg, 33 (in Russian).
Badalyan, O.G., Obridko, V.N., Sýkora, J.: 2005a, *Astron. Zh.* **82**, 535 (English translation *Astron. Rep.* **49**, 477).
Badalyan, O.G., Obridko, V.N., Sykora, J.: 2005b, In: Danesy, D., Poedts, S., De Groof, A., Andries, J. (eds.) *The Dynamic Sun: Challenges for Theory and Observations*, *Proc. 11-th European Solar Physics Meeting, ESA SP-600*, 152.1 (in CDROM).
Badalyan, O.G., Obridko, V.N., Rybak, J., Sykora, J.: 2003, In: Wilson, A. (ed.) *Solar Variability as an Input to the Earth's Environment*, *Proc. ISCS 2003, ESA SP-535*, 63.
Badalyan, O.G., Obridko, V.N., Rybák, J., Sýkora, J.: 2005, *Astron. Zh.* **82**, 740 (English translation *Astron. Rep.* **82**, 659).
Bai, T.: 1990, *Astrophys. J.* **364**, L17.
Ballester, J.L., Oliver, R., Carbonell, M.: 2005, *Astron. Astrophys.* **431**, L5.
Belvedere, G., Kuzanyan, K.M., Sokoloff, D.: 2000, *Monthly Noticies Roy. Astron. Soc.* **315**, 778.
Carbonell, M., Oliver, R., Ballester, J.L.: 1993, *Astron. Astrophys.* **274**, 497.
Chatfield, C.: 1989, *The Analysis of Time Series: An Introduction*, 4th edn., Chapman and Hall, London.
Gilman, D.L., Fuglister, F.J., Mitchell, J.M. Jr.: 1963, *J. Atmos. Sci.* **20**, 182.
Duchlev, P.I.: 2001, *Solar Phys.* **199**, 211.
Dziewoński, A., Bloch, S., Landisman, M.: 1969, *Bull. Seismol. Soc. Am.* **59**, 427.
Garcia, H.A.: 1990, *Solar Phys.* **127**, 185.
Gigolashvili, M.S., Japaridze, D.R., Mdzinarishvili, T.G., Chargeishvili, B.B.: 2005, *Solar Phys.* **227**, 27.
Hansen, R., Hansen, S.: 1975, *Solar Phys.* **44**, 225.
Howard, R.: 1974, *Solar Phys.* **38**, 59.
Jenkins, G.M., Watts, D.G.: 1968, *Spectral Analysis and Its Applications*, Holden-Day, London.
Knaack, R., Stenflo, J.O., Berdyugina, S.V.: 2004, *Astron. Astrophys.* **418**, L17.
Knaack, R., Stenflo, J.O., Berdyugina, S.V.: 2005, *Astron. Astrophys.* **438**, 1067.
Knoška, S.: 1985, *Contrib. Astron. Obs. Skalnaté Pleso* **13**, 217.
Li, K.J., Schmieder, B., Li, Q.-Sh.: 1998, *Astron. Astrophys.* **131**, 99.
Li, K.J., Yun, H.S., Gu, X.M.: 2001, *Astrophys. J.* **554**, L115.
Li, K.J., Wang, J.X., Xiong, S.Y., Liang, H.F., Yun, H.S., Gu, X.M.: 2002, *Astron. Astrophys.* **383**, 648.
Mariş, J., Popescu, M.D., Mierla, M.: 2002, *Rom. Astron. J.* **12**, 131.
Nagovitsyn, Yu.A.: 1998, *Izv. Gl. Astron. Obs.* **212**, 145 (in Russian).
Newton, H.W., Milsom, A.S.: 1955, *Monthly Noticies Roy. Astron. Soc.* **115**, 398.
Obridko, V.N., Gaziev, G.: 1992, In: Harvey, K.L. (ed.) *The Solar Cycle, Astron. Soc. Pacific Conf. Ser.* **27**, 410.
Obridko, V.N., Shelting, B.D.: 2001, *Astron. Zh.* **78**, 1146 (English translation *Astron. Rep.* **45**, 1012).
Oliver, R., Ballester, J.L.: 1994, *Solar Phys.* **152**, 481.
Özgüç, A., Üçer, C.: 1987, *Solar Phys.* **114**, 141.
Roy, J.R.: 1977, *Solar Phys.* **52**, 53.
Rušin, V.: 1980, *Bull. Astron. Inst. Czechoslov.* **31**, 9.
Rybák, J., Sýkora, J.: 2006, *Abstract Book, IAU 26-th General Assembly*, 323.
Storini, M., Sýkora, J.: 1997, *Nuovo Cimento* **20C**, 923.
Swinson, D.B., Koyama, H., Saito, T.: 1986, *Solar Phys.* **106**, 35.
Sýkora, J.: 1971, *Bull. Astron. Inst. Czechoslov.* **22**, 12.
Sýkora, J., 1980, In: Dryer, M., Tandberg-Hanssen, E. (eds.) *Solar and Interplanetary Dynamics, IAU Symp.* **91**, 87.
Sýkora, J., Rybák, J.: 2005, *Adv. Space Res.* **35**, 393.
Thomson, D.J.: 1982, *Proc. IEEE* **70**, 1055.
Tritakis, V.P., Mavromichalaki, H., Petropoulos, B.: 1988, *Solar Phys.* **115**, 367.
Verma, V.K.: 1987, *Solar Phys.* **114**, 185.
Verma, V.K., Pande, M.C., Uddin, W.: 1987, *Solar Phys.* **112**, 341.
Vitinskii, Yu.I., Kopecký, M., Kuklin, G.V.: 1986, *Statistics of Spot-Formation Activity of the Sun*, Nauka, Moscow (in Russian).
Vizoso, G., Ballester, J.L.: 1990, *Astron. Astrophys.* **229**, 540.
Waldmeier, M.: 1957, *Z. Astrophys.* **43**, 149.
Waldmeier, M.: 1971, *Solar Phys.* **29**, 332.
Yadav, R.S., Badruddin, Mr., Kumar, S.: 1980, *Indian J. Radio Space Phys.* **9**, 155.